

Electronic, redox and charge transport properties of an unusual hybrid structure: a bis(septithiophene) bridged by a fused tetrathiafulvalene (TTF)†‡

Iain A. Wright,^a Peter J. Skabara,^{*a} John C. Forgie,^a Alexander L. Kanibolotsky,^a Blanca González,^{§b} Simon J. Coles,^c Salvatore Gambino^d and Ifor D. W. Samuel^d

Received 15th July 2010, Accepted 23rd September 2010

DOI: 10.1039/c0jm02293d

A hybrid tetrathiafulvalene–oligothiophene compound has been synthesised, in which the fulvalene unit is fused on both sides to an end-capped septithiophene oligomer. The compound (**1**) has been studied by cyclic voltammetry, UV-vis spectroelectrochemistry and X-ray crystallography. The properties of this material are compared to the half-unit (**9**), which lacks the TTF core and contains only one septithiophene chain. In the case of the larger molecule, there are multiple and complex redox processes leading to the loss of 6–8 electrons per molecule. Charge generation layer time-of-flight measurements give maximum hole mobilities of *ca.* $1 \times 10^{-5} \text{ cm}^2 \text{ V}^{-1} \text{ s}^{-1}$.

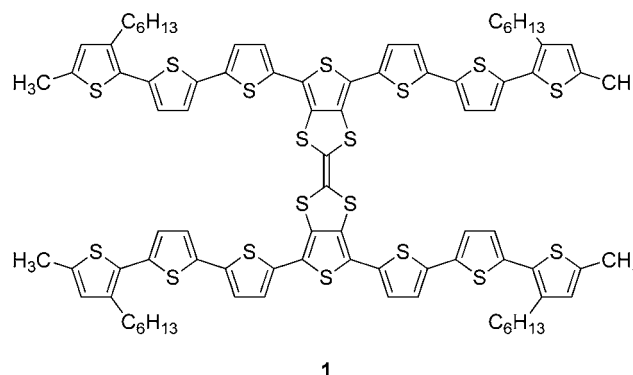
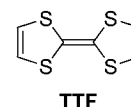
Introduction

By incorporating electron rich or deficient units into conjugated polymers and oligomers we have the potential to manipulate the HOMO and/or LUMO energy levels of the material, which is key to the development of semiconductor devices based upon polymer materials.^{1–3} Tetrathiafulvalene (TTF) derivatives have been the focus of ongoing research towards the development of new functional materials, largely due to its reliable redox behaviour and the metallic conductivity or superconductivity observed in its charge-transfer salts.^{4–9} Oligothiophenes are semiconducting species which have been intensively studied towards the generation of many new organic electronic devices, including light emitting diodes, field effect transistors and solar cells.^{2,10–14}

TTF derivatives have been studied as components in field-effect transistors and there are several examples of materials with high mobilities, including thiophene–TTF hybrids.^{15–19} In recent years we have been investigating oligothiophenes and polythiophenes that possess TTFs^{20–25} and other redox active systems^{26–30} fused directly to the backbone of the conjugated chain. Our interests arise from the complex redox behaviour resulting from the merging of two strong redox-active components. From these studies, we have found that, depending on the nature of the polymer, the fulvalene unit can either dominate the

electroactivity of the polymer or participate in a hybrid redox state.²² End-capped oligothiophenes are particularly attractive materials to study as they usually give well-defined redox signatures and stable charged intermediates,^{23,31} allowing for more precise analysis of the complex electrochemical behaviour of these hybrid systems.

In our previous work, the molecules developed bore TTF units stemming from the polythiophene chain and the signature of the TTF redox characteristics was clearly evident in electrochemical studies. In all these cases, the TTF system was fused directly to the conjugated chain through only one of the 1,3-dithiole rings, thereby retaining the signature oxidation of the second dithiole unit as an independent redox-active moiety. Here we report the synthesis and electrochemical study of a new hybrid molecule, featuring a TTF core fused at both ends of the molecule between two methyl end-capped septithiophene (7T) chains (**1**). The 7T chains also bear hexyl groups on the 3-position of the terminal thiophene rings to provide solubility.



^aWestCHEM, Department of Pure and Applied Chemistry, University of Strathclyde, Glasgow, G1 1XL, UK. E-mail: peter.skabara@strath.ac.uk

^bDepartamento de Química Inorgánica, Facultad de Ciencias, Universidad Autónoma de Madrid, Cantoblanco, 28049 Madrid, España

^cSchool of Chemistry, University of Southampton, Highfield, Southampton, SO17 1BJ, UK

^dOrganic Semiconductor Centre, SUPA, School of Physics & Astronomy, University of St Andrews, St Andrews, KY16 9SS, UK

† Electronic supplementary information (ESI) available: Full experimental details for the synthesis of all new compounds and crystallographic data. CCDC reference numbers 783815, 783816. For ESI and crystallographic data in CIF or other electronic format see DOI: 10.1039/c0jm02293d

‡ This paper is part of a *Journal of Materials Chemistry* themed issue in celebration of the 70th birthday of Professor Fred Wudl.

§ Present address: Departamento de Química Inorgánica y Bioinorgánica, Facultad de Farmacia, Universidad Complutense de Madrid, Ciudad Universitaria, Madrid 28040, España.

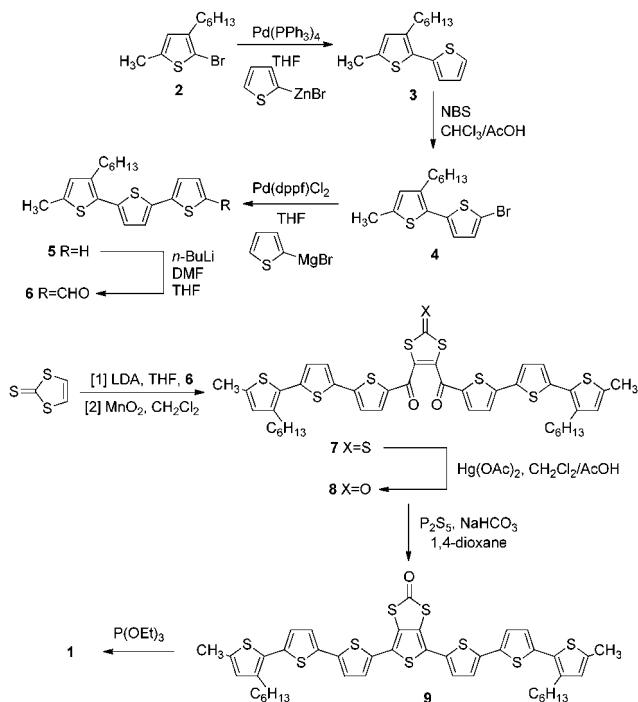
Results and discussion

Synthesis

The strategy employed for the synthesis of **1** is shown in Scheme 1. 2-Bromo-3-hexyl-5-methylthiophene (**2**) can be made by treating 3-hexylthiophene first with NBS to give 2-bromo-3-hexylthiophene (98% yield),³² followed by methylation using LDA/iodomethane to give **2** in 91% yield. This procedure is different to the one reported by Sato and Kamine,³³ who performed methylation of 3-hexylthiophene before bromination, to obtain an overall yield of 36% for compound **2**. Negishi coupling of **2** with 2-thienylzinc bromide affords bithiophene **3** in 67% yield. Subsequent bromination to generate **4** is achieved easily and efficiently with NBS (96% yield), prior to Kumada coupling with thiophen-2-yl magnesium bromide to obtain **5** in 88% yield. Carbonylation with *n*-BuLi/DMF generates the desired terthiophene aldehyde **6** in 83% yield. Two-fold sequential lithiation of vinylene trithiocarbonate, followed by the addition of **6**, gave the corresponding diol intermediate, which was oxidised immediately with MnO₂ to afford the 1,3-dithiole-2-thione **7** with an overall yield of 60%. Transchalcogenation of the 1,3-dithiole-2-thione to the carbonyl derivative (**8**) was achieved in almost quantitative yield with mercuric acetate. Paal–Knorr thiophene synthesis using P₂S₅ was applied to yield the TTF precursor **9** (69% yield). Finally, homocoupling of **9** with triethylphosphite at 125°C afforded the TTF compound **1** in 39% yield.

Electrochemistry

In order to investigate the electrochemical properties and consequences of fusing TTF directly between the 7T chains, cyclic voltammetry experiments were performed on compounds **1**



Scheme 1 Synthesis of the TTF-bis(septithiophene) **1** and its 1,3-dithiole-2-one precursor **9**.

and **9** (Fig. 1 and Table 1). The oxidation of **9** shows three sequential oxidation waves. The first two occur at half-wave potentials of +0.44 and +0.64 V and these values are quite close for the oxidation to the radical cation and to the dication intermediates, respectively. The third wave appears at +1.02 V, affording a radical trication. All three oxidation processes are reversible or quasi-reversible. The electrochemical stability is a consequence of the α -methyl groups on the terminal thiophenes, which impede any coupling reactions to generate a polymeric species. In comparison to end-capped sextithiophene derivatives that we have made previously (**10** and **11**, in which only dications were accessible),³¹ the extended septithiophene **9** allows access to an additional redox state.

Though the presence of the TTF core in **1** may lead us to expect two discernible reversible waves in the corresponding cyclic voltammogram, the oxidation of **1** in fact shows a complex series of redox processes over a wide potential range. The data are given in Table 1, but it is difficult to explain and interpret the results with a high level of confidence. It is reasonable to assume that the additional peak for **1**, seen at the half-wave potential of

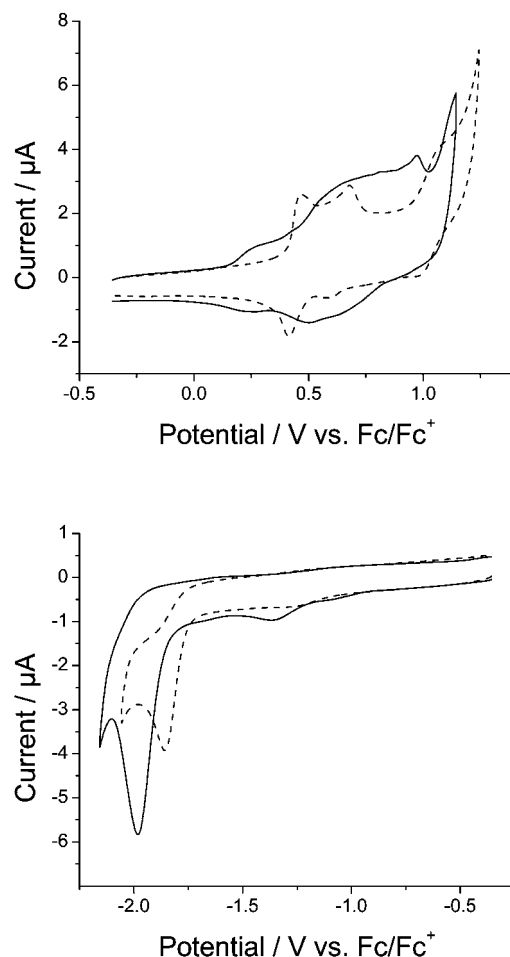


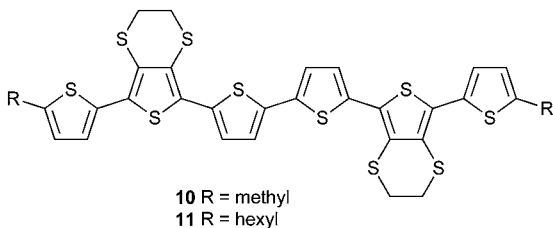
Fig. 1 Cyclic voltammograms of TTF derivative **1** (solid line) and half-unit **9** (dashed line) for oxidation (top) and reduction (bottom) in dichloromethane solution, using a carbon working electrode, Ag wire pseudo-reference electrode, TBAPF₆ (0.1 M) as the supporting electrolyte, substrate concentration 10⁻⁴ M, scan rate 100 mV s⁻¹. The data are referenced to the ferrocene/ferrocenium redox couple.

Table 1 Electronic absorption and electrochemical data

	Compound 1	Compound 9
$\lambda_{\text{max}}/\text{nm}$ (CH_2Cl_2)	461	467
HOMO–LUMO gap ^a /eV	2.20	2.29
$E_{1\text{ox}}/\text{V}$ (CH_2Cl_2)	+0.26/+0.23	+0.47/0.41
$E_{2\text{ox}}/\text{V}$ (CH_2Cl_2)	+0.66/+0.49 ^d	+0.68/+0.59 ^d
$E_{3\text{ox}}/\text{V}$ (CH_2Cl_2)	+0.97/+0.94 ^d	+1.05/+0.98 ^d
E_{red}/V (CH_2Cl_2)	−1.98 ^e	−1.86 ^e
HOMO/eV ^b	−4.95	−5.18
LUMO/eV ^b	−3.00	−3.08
HOMO–LUMO gap ^c /eV	1.95	2.10

^a Optical HOMO–LUMO gap calculated from the onset of the longest wavelength absorption maximum. ^b HOMO and LUMO levels are calculated from the onset of the first peak of the corresponding redox wave and are referenced to ferrocene which has a HOMO of −4.8 eV. ^c Electrochemical HOMO–LUMO gap. ^d Quasi-reversible peak. ^e Irreversible peak.

+0.25 V, suggests the oxidation of the TTF unit. However, further studies cast a doubt on such an assignment (*vide infra*). In general, differential pulse voltammetry normally provides better resolution of redox processes, but for compound **1** no further insight into the complex nature of the redox chemistry could be made. For the purpose of a more accurate electrochemical analysis, we are currently in the process of synthesising quinque thiophene and terthiophene analogues of **1**, since these compounds will serve to simplify the redox characteristics of the hybrid system sequentially, down to the TTF core.³⁴



Cyclic voltammograms depicting the reduction of **1** and **9** show irreversible peaks at −2.10 and −1.80 V respectively, due to the formation of radical anions in the septithiophene chains. The small peaks at *ca.* −1.3 V are due to oxygen present in the electrolytic solution.

The electrochemical HOMO–LUMO gaps of the materials were obtained from the difference in the onsets of the first oxidation and reduction peaks (Table 1). Using data referenced to the ferrocene/ferrocenium redox couple, HOMO and LUMO energies were calculated by subtracting the onsets from the HOMO of ferrocene, which has a known value of −4.8 eV. The electrochemical HOMO–LUMO gaps of **1** and **9** were 1.95 and 2.10 eV, respectively, and are a little lower than the optical data (see the following section).

Spectroelectrochemistry

The absorption spectra of compounds **1** and **9** (Fig. 2) demonstrate peak maxima at 461 and 467 nm, respectively, due to the π – π^* transitions of the individual septithiophene chains. These values are slightly red-shifted compared to an unsubstituted cruciform bis(septithiophene) reported by Scherf *et al.* (451 nm in chloroform solution).³⁵ This difference in absorption

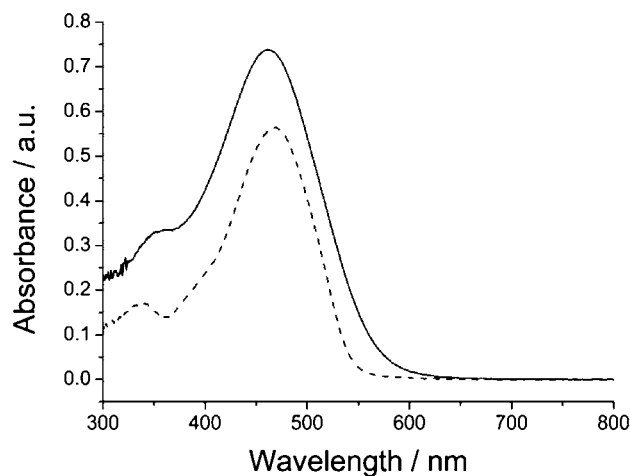


Fig. 2 Absorption spectra of compounds **1** (solid line) and **9** (dashed line) in dichloromethane solution.

wavelengths is due to the electronic effects of the alkyl and sulfur substituents in compounds **1** and **9**. It is worth noting that the fused TTF unit does not provide a conjugated link between the oligothiophene chains in **1**. However, the TTF and 1,3-dithiole-2-one units in **1** and **9** are responsible for the shortest wavelength peaks at 353 and 338 nm, respectively.²⁴ The onset of the longest wavelength absorption edge gives the optical HOMO–LUMO gap of **1** and **9** at 2.20 and 2.29 eV, respectively.

The solid state spectrum of compound **9** (Fig. 3) is very similar to the end-capped sexithiophenes **10** and **11**.³¹ The absorption band is red-shifted compared to the solution state spectrum, with peaks at 495 and 561 nm (λ_{max} for **10** = 481, 510 and 551 nm). As in **10** and **11**, the tail of the absorption band for compound **9** extends over several hundred nm. Solid state UV-vis spectroelectrochemistry (SEC) of **9** also follows a similar trend to those seen for compounds **10** and **11**. A broad band forms between 670 and 930 nm at potentials higher than +0.5 V, together with a band >1100 nm. Throughout the experiment, the main π – π^* band remains unchanged, but the broad band that evolves on oxidation superimposes the original band. Noticeably, there is a trough in the spectrum of the oxidised compound at about 930 nm and this is pertinent to the SEC plot for compound **1**.

The absorption spectrum for the film of compound **1** (Fig. 3) gives a peak at 496 nm, a bathochromic shift of 29 nm compared to the solution state spectrum. Upon oxidation, a small band appears at 933 nm at *ca.* +0.3 V. This peak is typical for the oxidation of a TTF species to the radical cation and can be assigned to intermolecular charge transfer between TTF^{•+} dimers.²⁴ The peak is quickly lost upon further oxidation and is eclipsed by a band with a peak maximum at 597 nm and a second band at >1100 nm. The trough observed for compound **9** is not evident in **1** due to the signature of oxidised TTF over this region of the spectrum. Furthermore, it is interesting to note that the π – π^* band for the neutral compound diminished upon oxidation and that there is a clear isosbestic point at 521 nm. For both compounds, the films dissolve into solution at higher potentials, due to the solubility of the multi-charged states. These results, in combination with the cyclic voltammetry data, indicate that the first site of oxidation in **1** involves the TTF unit.

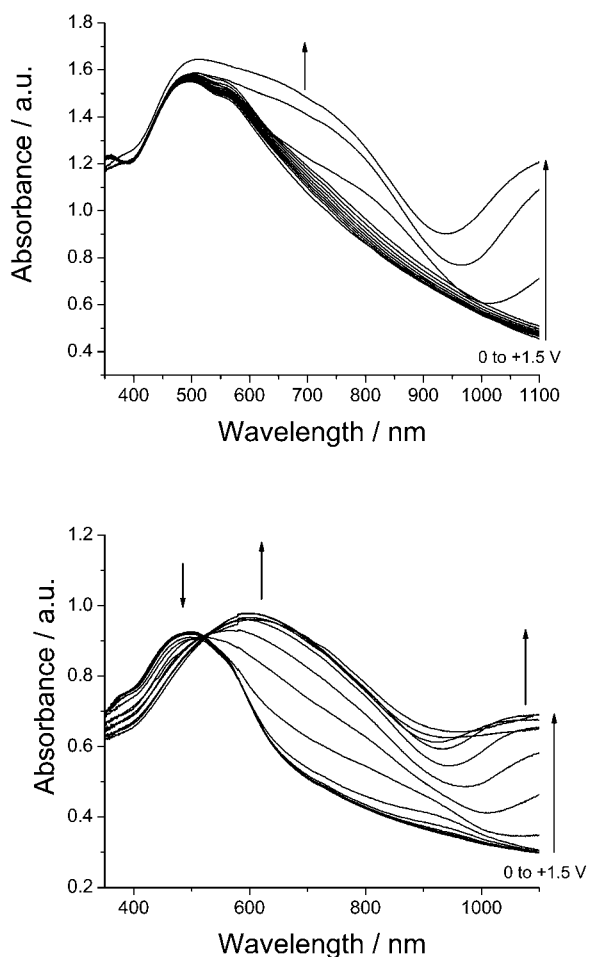


Fig. 3 Solid state UV-vis spectroelectrochemistry of thin films of the TTF half unit **9** (top) and fused TTF system **1** (bottom). Thin films were deposited onto ITO slides *via* drop-casting. Measurements were performed with a Pt counter electrode and a pseudo-Ag reference in monomer free acetonitrile solution containing TBAPF₆ (0.1 M) as the supporting electrolyte.

Although the solution and solid state absorption spectra did not show any signs of doping, we obtained the EPR spectra for compounds **1** and **9** to investigate the presence of radicals. In both cases, we obtained peaks at $g = 2.0046$ (compound **1**) and 2.0050 (compound **9**), indicating that the materials carry residual radical cations. In comparison to these values, thiophene radicals give values in the region of 2.002 – 2.003 , whilst TTF radical cations have g values of *ca.* 2.008 .³⁶ For hybrid TTF–polythiophene materials, we have observed $g = 2.0078$ for a polymer in which the electroactivity is concentrated solely within the TTF units,²⁴ and values of around 2.005 for structures in which the radical cation is delocalised over the thiophene–dithiole units.²² Our results for compounds **1** and **9** are commensurate with hybrid electroactivity, but it is surprising that the dithiole-2-one heterocycle is involved with the cation radical.

Crystallography

Crystals of the TTF derivative were grown by slow evaporation from a chloroform–carbon disulfide solution and isolated as a 1 : 1 carbon disulfide solvate. The molecular structure of

compound **1** is shown in Fig. 4a. The asymmetric unit is defined by the ring systems labelled A–H and the molecule has an inversion centre around the central double bond of the TTF unit. The dithienoTTF fragment is essentially planar, but there is a significant twisting in one end of the septithiophene chain, most likely due to packing forces. The dihedral angle between rings A and B is 33° and the two thiophenes adopt a *syn* conformation. Conjugation is weakest in this portion of the molecule and the dihedral angles between rings B–C and C–D are 11° and 16° , respectively. In contrast, the dihedral angles between thiophenes D–G are in the range 4 – 10° . The sextithiophene fragment represented by B–G adopts an *anti* conformation. The stacked packing structure of compound **1** is shown in Fig. 4b and the overlap between chains within each stack, identifying the closest interactions, is depicted in Fig. 4c. The angle between the two planes of rings D and F is $5.79(12)^\circ$ and the distance between these planes is $3.738(2)$ Å. There is a larger angle between the planes of thiophenes C and G ($18.36(12)^\circ$), but the two sulfur atoms of the corresponding rings show a weak non-covalent interaction with a S···S distance of $3.811(1)$ Å. Given the greater degree of twist in A and B, it is perhaps not surprising that these rings do not participate in the stacking mode of compound **1**.

Crystals of compound **9** were obtained from a hot dichloromethane/hexane solution. Once again, the septithiophene adopts an all-*anti* conformation apart from one terminal thiophene ring (Fig. 5a). The range of dihedral angles between the *anti*-thiophenes is 6 – 19° , and the angle between the two *syn* thiophenes is 26° . The molecule packs in a stacked herringbone pattern (Fig. 5b). Within the stacks, the 1,3-dithiole ring is associated with ring-over-bond overlap with one adjacent molecule (interplanar distance of 3.57 Å), and π – π overlap with the terminal *syn* thiophene ring of the second molecule (interplanar distance of 3.38 Å, Fig. 5c).

DFT calculations

Density functional theory was applied to **1** to gain a better understanding of the electronic energy levels within the compound. The calculations were performed with Spartan 08, using the B3LYP hybrid functional with a 6-31G* basis set. Firstly, a single point energy calculation was performed on the structure obtained by X-ray analysis, with the hexyl groups replaced by methyl groups. Secondly, the terminal bithiophene units with the *syn* conformation were twisted to an *anti* orientation and this structure was allowed to relax to a local minimum. The calculated HOMO–LUMO gap for the all-*anti* conformer (2.49 eV) was found to be closer to the experimental HOMO–LUMO gap (Table 1), than the structure obtained from crystallography (2.70 eV). Also, the all-*anti* conformer was lower in energy, showing that this is the preferred geometry in the gas phase. The orbitals of **1** as the all-*anti* conformer are depicted in Fig. 6 and show that the HOMO is derived from the oligothiophene chain. The TTF is involved with the HOMO-2 orbital, but this energy level is only 0.17 eV deeper than the HOMO. It is entirely feasible that the first oxidation state of this material involves both components and a more in-depth computational study will be performed to help elucidate the complex redox chemistry of this material.

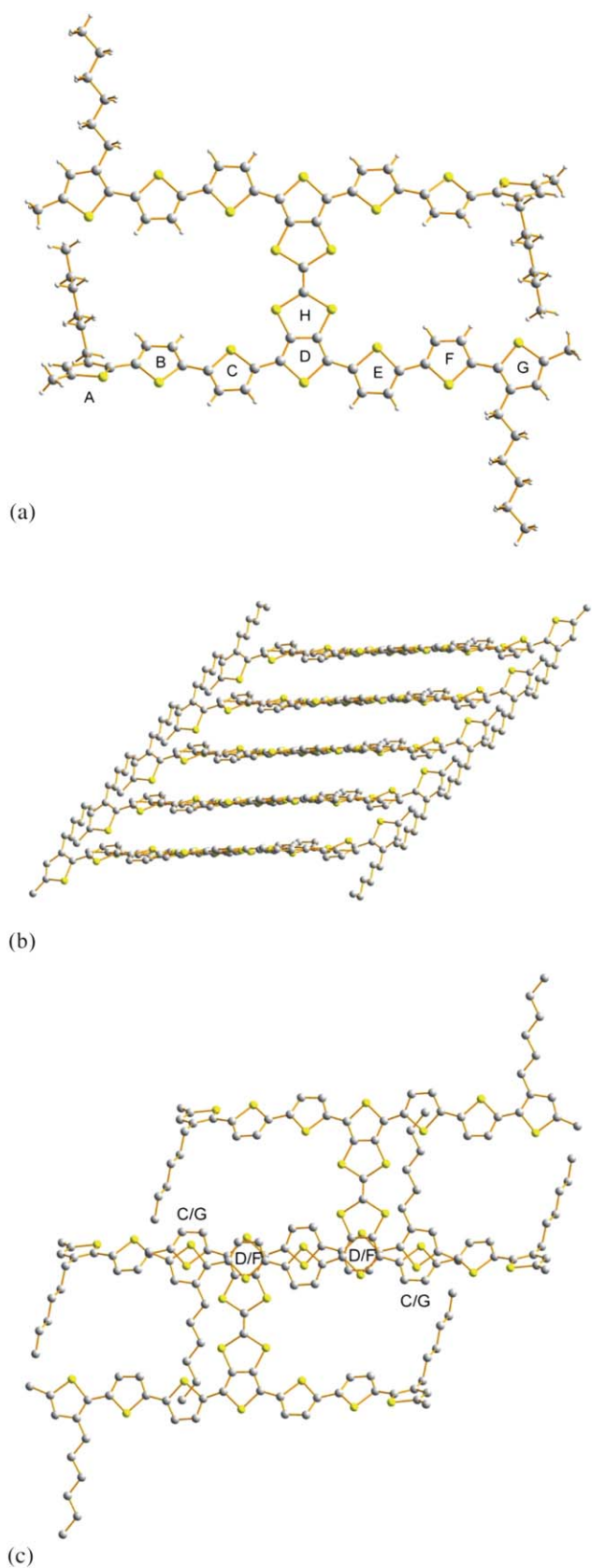


Fig. 4 (a) Molecular structure of compound **1**; (b) stacking of molecules through π -interactions; (c) overlap of rings viewed down a stack.

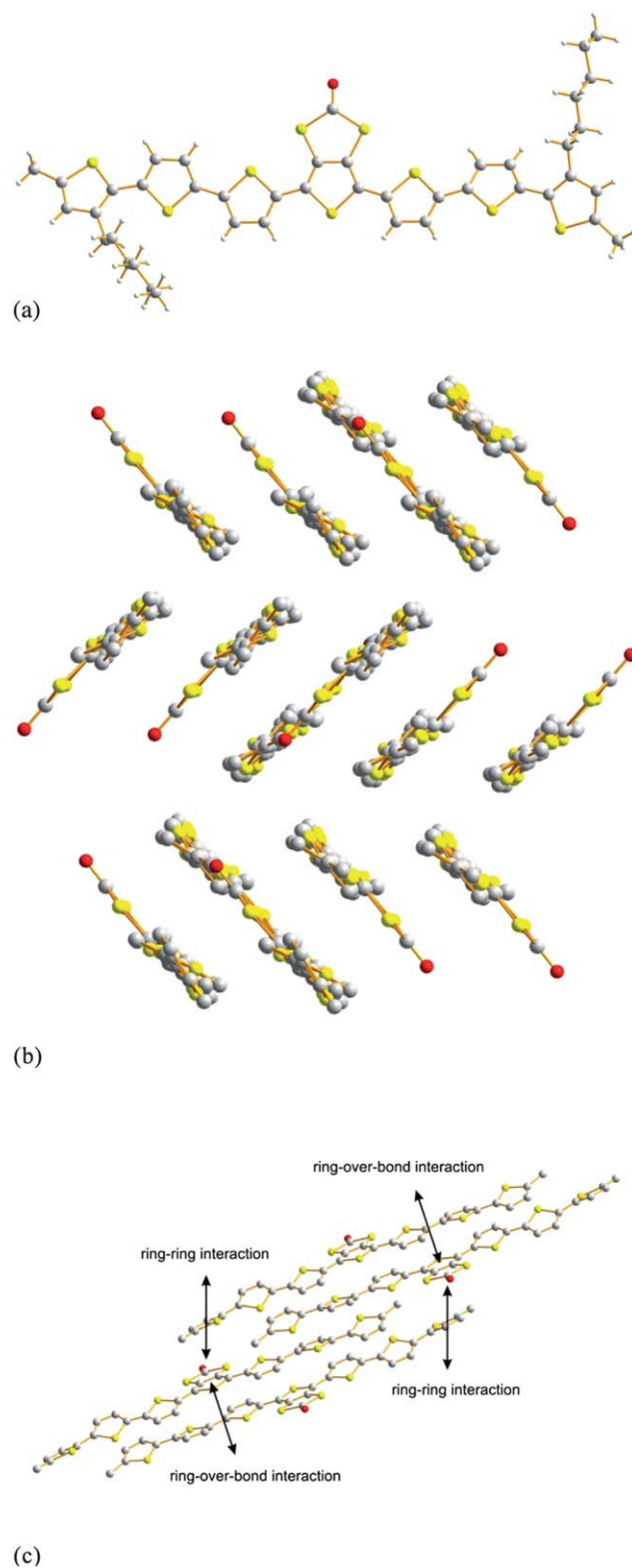


Fig. 5 (a) Molecular structure of compound **9**; (b) herringbone orientation of stacks; (c) overlap of rings within the stacks.

Time-of-flight measurements

We have seen so far the electronic and redox properties of compounds **1** and **9**. We now move to the study of their charge

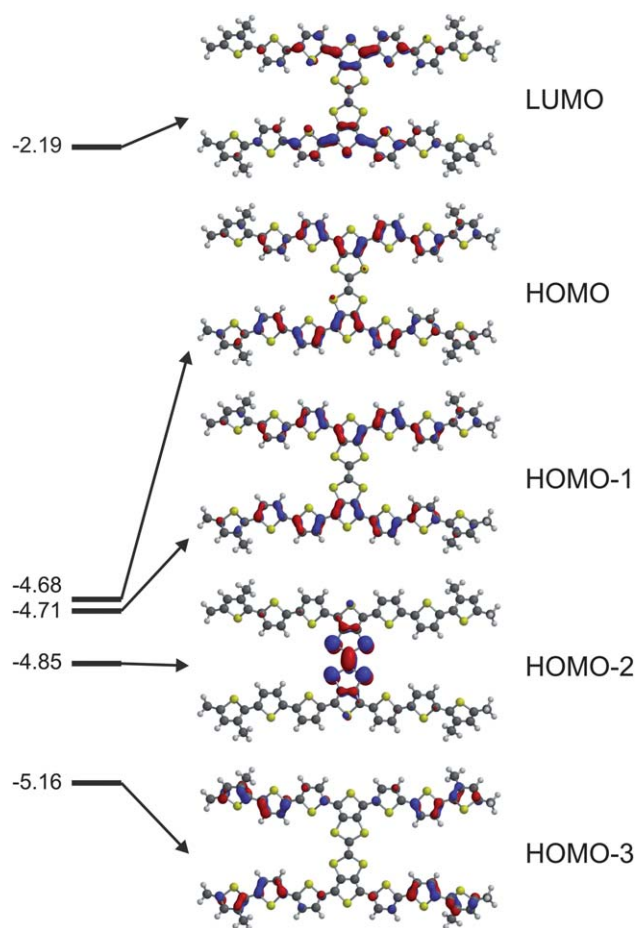


Fig. 6 Selected molecular orbitals of compound 1.

transport properties. We performed charge generation layer time-of-flight (CGL-TOF) measurements on compounds **1** and **9**. For these measurements, solutions of the two compounds were made to concentrations of about 40 mg ml⁻¹ in chlorobenzene : carbon disulfide (1 : 1). Films were spin-coated onto an ITO substrate at speeds of 1000 rpm to obtain films around 200–230 nm thick. CGL-TOF experimental details have been already reported in ref. 37.

Fig. 7 shows the hole photocurrent transient on linear and log–log scales for a film of compound **1**, at room temperature and for an applied electric field $E = 2.5 \times 10^5$ V cm⁻¹. The absence of a clear plateau in the photocurrent transient on a linear scale is indicative of highly dispersive charge transport behaviour. In order to estimate the transit time (t_{tr}) a log–log plot was necessary, which allowed measurement of the transit time from the change of slope of the photocurrent transient, $t_{tr} = 18$ μ s. The transit time corresponds to a mobility of 4.4×10^{-6} cm² V⁻¹ s⁻¹.

For a direct comparison, CGL-TOF measurements were performed on compound **9** under the same conditions, such as temperature and electric field. Fig. 8 shows the hole photocurrent transient on linear and log–log scales for a film of compound **9**, at room temperature and for an applied electric field $E = 2.5 \times 10^5$ V cm⁻¹. Again the absence of a clear plateau in the photocurrent transient on a linear scale is indicative of highly dispersive charge transport behaviour and a log–log plot was necessary to estimate

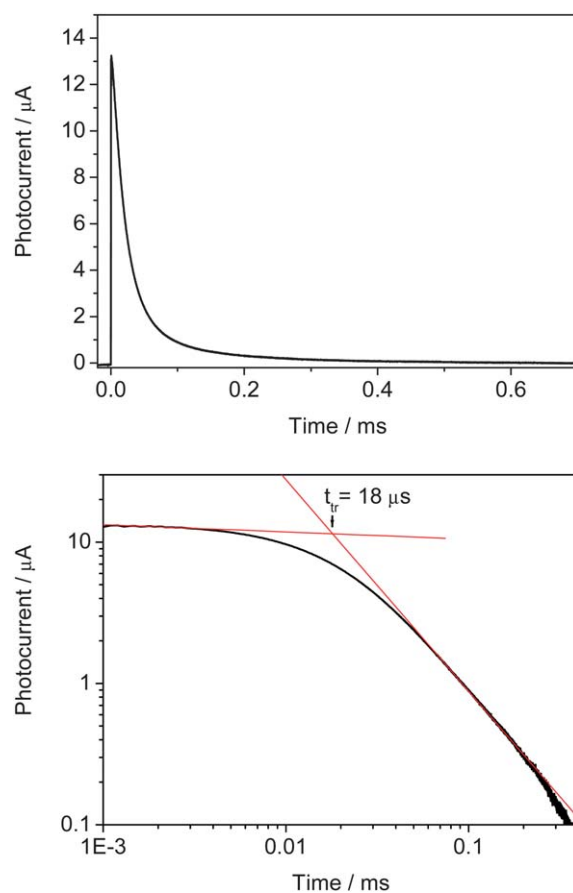


Fig. 7 Hole photocurrent transient on linear (top) and log–log scale (bottom) for a film of compound **1**, at room temperature and for an applied electric field $E = 2.5 \times 10^5$ V cm⁻¹.

the transit time ($t_{tr} = 62$ μ s). The transit time corresponds to a mobility of 1.4×10^{-6} cm² V⁻¹ s⁻¹.

Compound **1** shows hole mobility values three times higher than compound **9** under the same electric field and this is consistent with improved molecular orbital overlap between the larger oligothiophene–TTF molecules.

Several examples of TTF derivatives have been reported so far in the literature with mobilities up to 3.6 cm² V⁻¹ s⁻¹ for OFET single crystal devices.^{9,16,17,38} OFET single crystals are found to give the highest mobilities largely due to their regular molecular ordering that permits extensive intermolecular overlap to occur.³⁹ Most attention has been placed so far on improving the mobility of OFETs based on TTF derivatives, but not so much has been reported on charge transport measurements in the direction perpendicular to the substrate. This is a concern because some important optoelectronic devices, namely solar cells and organic memory devices based on TTF-based materials, have been reported already in the literature^{22,40} and they require charge transport in the direction perpendicular to the substrate. Thus an insight into mobility values would be useful for these applications.

Our measurements give the hole mobility in the direction perpendicular to the substrate, and we have studied its field dependence, as shown in Fig. 9. As the electric field is increased from 2.5×10^5 to 7.4×10^5 V cm⁻¹, the hole mobility increases

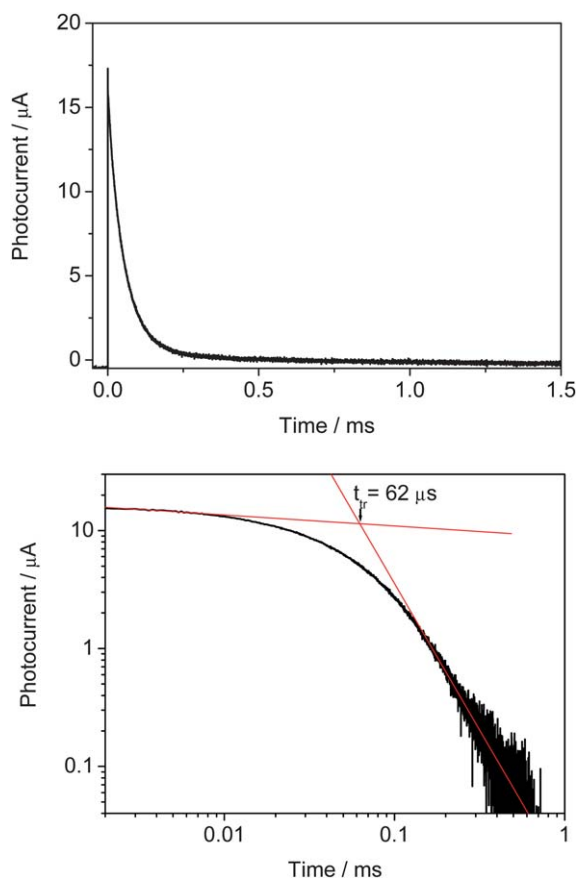


Fig. 8 Hole photocurrent transient on linear (top) and log–log scale (bottom) for a film of compound **9**, at room temperature and for an applied electric field $E = 2.5 \times 10^5 \text{ V cm}^{-1}$.

from 1.4×10^{-6} to $1.3 \times 10^{-5} \text{ cm}^2 \text{ V}^{-1} \text{ s}^{-1}$ for compound **9**. For compound **1** as the electric field is increased from 1×10^5 to $4 \times 10^5 \text{ V cm}^{-1}$, the hole mobility increases from 1.4×10^{-6} to $1.1 \times 10^{-5} \text{ cm}^2 \text{ V}^{-1} \text{ s}^{-1}$. Fig. 9 shows that both materials exhibit similar electric field mobility dependence.

We clearly see that mobility values are several orders of magnitude less when charge transport is measured in the

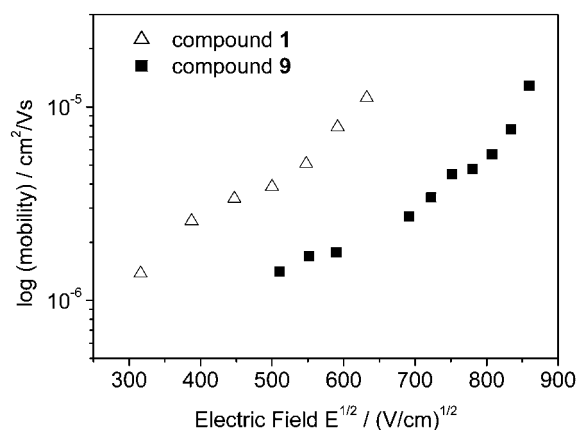


Fig. 9 Room temperature mobility vs. electric field for the two compounds investigated.

direction normal to the substrate instead of parallel to the plane. It is difficult to compare charge transport properties between the two methods, because our compounds clearly differ in size and complexity from the ones previously reported for FET mobility measurements. Furthermore, as has been reported for P3HT, TOF mobility values can be orders of magnitude lower than FET mobilities.^{41–43}

Our mobility values are consistent with others previously reported using TOF or CELIV techniques on a related family of thiophene-based conjugated materials.^{37,44,45} In this work, CGL-TOF measurements have shown that it is possible to tune the energy (HOMO–LUMO) levels without inhibiting the charge transport properties of the thiophene oligomers. In fact, the thiophene semiconducting properties are similar to previously reported thiophene-based materials. The OFET characteristics of these materials will be reported elsewhere.

Summary

A new hybrid TTF-thiophene material (**1**) has been synthesised and its electrochemical and electronic properties have been investigated and compared to the ‘non-TTF’ half-unit. As we have seen in polymeric systems, a close and intimate association of the TTF unit with the thiophene chain leads to hybrid electroactivity and complex redox chemistry. The charge transport properties of compounds **1** and **9** do not differ greatly, but the HOMO energy level of the TTF compound is closer to vacuum than the dithiole derivative as the former is a stronger electron donor. Compound **1** has mobility a factor of three higher than compound **9** (at a field of $2.5 \times 10^5 \text{ V cm}^{-1}$) due to improved molecular orbital overlap. The presence of the TTF unit in **1** affords additional redox states and it is proposed that up to eight electrons are removed from this material within a narrow potential window. Such highly redox-active materials are promising for application in technologies such as solar cells, batteries or capacitors.

Acknowledgements

ALK, IAW, SG and IDWS thank the EPSRC for funding. IAW is grateful to Will Skene (Université de Montréal) for time spent in his laboratory during the course of this work, funded by the JCEMolChem programme. PJS thanks Andrey Moiseev (University of McGill) for conducting EPR measurements.

Dedicated to Fred Wudl for his enthusiasm and encouragement towards complex and unusual electroactive organic structures.

Notes and references

- 1 J. C. Forgie, P. J. Skabara, I. Stibor, F. Vilela and Z. Vobecka, *Chem. Mater.*, 2009, **21**, 1784.
- 2 A. Mishra, C.-Q. Ma and P. Bäuerle, *Chem. Rev.*, 2009, **109**, 1141.
- 3 *Handbook of Thiophene-based Materials: Applications in Organic Electronics and Photonics*, ed. I. F. Perepichka and D. F. Perepichka, John Wiley & Sons, Chichester, 2009.
- 4 E. Coronado and P. Day, *Chem. Rev.*, 2004, **104**, 5419.
- 5 P. Frère and P. J. Skabara, *Chem. Soc. Rev.*, 2005, **34**, 69.
- 6 D. Jerome, *Chem. Rev.*, 2004, **104**, 5565.
- 7 C. Rovira, *Chem. Rev.*, 2004, **104**, 5289.
- 8 J. Yamada, H. Akutsu, H. Nishikawa and K. Kikuchi, *Chem. Rev.*, 2004, **104**, 5057.

- 9 N. Gautier, M. Cariou, A. Gorgues and P. Hudhomme, *Tetrahedron Lett.*, 2000, **41**, 2091.
- 10 A. R. Murphy and J. M. J. Frechet, *Chem. Rev.*, 2007, **107**, 1066.
- 11 I. F. Perepichka, D. F. Perepichka, H. Meng and F. Wudl, *Adv. Mater.*, 2005, **17**, 2281.
- 12 M. Mazzeo, D. Pisignano, L. Favaretto, G. Barbarella, R. Cingolani and G. Gigli, *Synth. Met.*, 2003, **139**, 671.
- 13 A. B. Tamayo, B. Walker and T. Q. Nguyen, *J. Phys. Chem. C*, 2008, **112**, 11545.
- 14 J. Roncali, *Chem. Soc. Rev.*, 2005, **34**, 483.
- 15 M. Mas-Torrent and C. Rovira, *Chem. Soc. Rev.*, 2008, **37**, 827.
- 16 M. Leufgen, O. Rost, C. Gould, G. Schmidt, J. Geurts, L. W. Molenkamp, N. S. Oxtoby, M. Mas-Torrent, N. Crivillers, J. Veciana and C. Rovira, *Org. Electron.*, 2008, **9**, 1101.
- 17 X. K. Gao, W. F. Qiu, Y. Q. Liu, G. Yu and D. B. Zhu, *Pure Appl. Chem.*, 2008, **80**, 2405.
- 18 O. Aleveque, P. Frère, P. Leriche, T. Breton, A. Cravino and J. Roncali, *J. Mater. Chem.*, 2009, **19**, 3648.
- 19 M. Mas-Torrent and C. Rovira, *J. Mater. Chem.*, 2006, **16**, 433.
- 20 A. L. Kanibolotsky, J. C. Forgie, S. Gordeyev, F. Vilela, P. J. Skabara, J. E. Lohr, B. M. Petersen and J. O. Jeppesen, *Macromol. Rapid Commun.*, 2008, **29**, 1226.
- 21 R. Berridge, P. J. Skabara, R. Andreu, J. Garin, J. Orduna and M. Torra, *Tetrahedron Lett.*, 2005, **46**, 7871.
- 22 R. Berridge, P. J. Skabara, C. Pozo-Gonzalo, A. Kanibolotsky, J. Lohr, J. J. W. McDouall, E. J. L. McInnes, J. Wolowska, C. Winder, N. S. Sariciftci, R. W. Harrington and W. Clegg, *J. Phys. Chem. B*, 2006, **110**, 3140.
- 23 A. L. Kanibolotsky, L. Kanibolotskaya, S. Gordeyev, P. J. Skabara, I. McCulloch, R. Berridge, J. E. Lohr, F. Marchioni and F. Wudl, *Org. Lett.*, 2007, **9**, 1601.
- 24 P. J. Skabara, R. Berridge, E. J. L. McInnes, D. P. West, S. J. Coles, M. B. Hursthouse and K. Mullen, *J. Mater. Chem.*, 2004, **14**, 1964.
- 25 P. J. Skabara, D. M. Roberts, I. M. Serebryakov and C. Pozo-Gonzalo, *Chem. Commun.*, 2000, 1005.
- 26 J. C. Forgie, A. L. Kanibolotsky, P. J. Skabara, S. J. Coles, M. B. Hursthouse, R. W. Harrington and W. Clegg, *Macromolecules*, 2009, **42**, 2570.
- 27 P. J. Skabara, R. Berridge, I. M. Serebryakov, A. L. Kanibolotsky, L. Kanibolotskaya, S. Gordeyev, I. F. Perepichka, N. S. Sariciftci and C. Winder, *J. Mater. Chem.*, 2007, **17**, 1055.
- 28 C. Pozo-Gonzalo, R. Berridge, P. J. Skabara, E. Cerrada, M. Laguna, S. J. Coles and M. B. Hursthouse, *Chem. Commun.*, 2002, 2408.
- 29 P. J. Skabara, I. M. Serebryakov, I. F. Perepichka, N. S. Sariciftci, H. Neugebauer and A. Cravino, *Macromolecules*, 2001, **34**, 2232.
- 30 P. J. Skabara, C. Pozo-Gonzalo, N. L. Miazza, M. Laguna, E. Cerrada, A. Luquin, B. Gonzalez, S. J. Coles, M. B. Hursthouse, R. W. Harrington and W. Clegg, *Dalton Trans.*, 2008, 3070.
- 31 C. R. Mason, P. J. Skabara, D. Cupertino, J. Schofield, F. Meghdadi, B. Ebner and N. S. Sariciftci, *J. Mater. Chem.*, 2005, **15**, 1446.
- 32 J. P. Lere-Porte, J. J. E. Moreau and C. Torrelles, *Eur. J. Org. Chem.*, 2001, 1249.
- 33 M. Sato and H. Kamine, *Chem. Lett.*, 2009, 924.
- 34 I. A. Wright, A. L. Kanibolotsky and P. J. Skabara, in preparation.
- 35 A. Bilge, A. Zen, M. Forster, H. B. Li, F. Galbrecht, B. S. Nehls, T. Farrell, D. Neher and U. Scherf, *J. Mater. Chem.*, 2006, **16**, 3177.
- 36 F. Gerson and W. Huber, *Electron Spin Resonance Spectroscopy of Organic Radicals*, Wiley-VCH, Weinheim, 2003.
- 37 G. J. McEntee, P. J. Skabara, F. Vilela, S. Tierney, I. D. W. Samuel, S. Gambino, S. J. Coles, M. B. Hursthouse, R. W. Harrington and W. Clegg, *Chem. Mater.*, 2010, **22**, 3000.
- 38 M. Mas-Torrent, M. Durkut, P. Hadley, X. Ribas and C. Rovira, *J. Am. Chem. Soc.*, 2004, **126**, 984.
- 39 S. T. Bromley, M. Mas-Torrent, P. Hadley and C. Rovira, *J. Am. Chem. Soc.*, 2004, **126**, 6544.
- 40 C. W. Chu, J. Ouyang, H. H. Tseng and Y. Yang, *Adv. Mater.*, 2005, **17**, 1440.
- 41 H. Sirringhaus, P. J. Brown, R. H. Friend, M. M. Nielsen, K. Bechgaard, B. M. W. Langeveld-Voss, A. J. H. Spiering, R. A. J. Janssen, E. W. Meijer, P. Herwig and D. M. de Leeuw, *Nature*, 1999, **401**, 685.
- 42 A. J. Mozer, N. S. Sariciftci, A. Pivrikas, R. Osterbacka, G. Juska, L. Brassat and H. Bassler, *Phys. Rev. B: Condens. Matter Mater. Phys.*, 2005, **71**, 035214.
- 43 K. Kaneto, K. Hatae, S. Nagamatsu, W. Takashima, S. S. Pandey, K. Endo and M. Rikukawa, *Jpn. J. Appl. Phys.*, 1999, **38**, L1188.
- 44 A. J. Mozer, C. Q. Ma, W. W. H. Wong, D. J. Jones, P. Bauerle and G. G. Wallace, *Org. Electron.*, 2010, **11**, 573.
- 45 T. C. Chao, K. T. Wong, W. Y. Hung, T. H. Hou and W. J. Chen, *Tetrahedron Lett.*, 2009, **50**, 3422.